A technique based on the equivalent source method for measuring the surface impedance and reflection coefficient of a locally reacting material

Yong-Bin ZHANG[1]; Wang-Lin LIN; Chuan-Xing BI

[1] Hefei University of Technology, China

ABSTRACT

A technique based on equivalent source method (ESM) is developed in this paper for measuring the surface impedance and reflection coefficient of a test material. The technique requires the measurement of complex pressures on two parallel planes between the sound source and the test material. If the sound source has rotational symmetry, the measurement on two parallel lines is sufficient. The sound pressure and normal component of particle velocity on the surface of the test material can then be calculated by using the ESM. The technique is similar to that proposed by Tamura in which the spatial Fourier transform rather than the ESM is used. Numerical examples are given to compare the proposed technique with the Tamura method, and the results show that a smaller measurement aperture is required and the measurement noises are easier to be controlled when using the proposed technique.

Keywords: Acoustic impedance, Reflection coefficient, Equivalent source method
I-INCE Classification of Subjects Number(s): 72.7

1. INTRODUCTION

Many methods for measuring the surface impedance and absorption coefficient of a test material in free field or in-situ have been developed. These methods can be classified into two major categories. The methods of the first category depend on the type of sound wave model, and there are so far three typical kinds of sound wave model: a) plane wave model; b) mirror model in which the spherical wave reflects as the plane wave; c) spherical wave model. Based on the plane wave model, the most famous method is the transfer function method proposed by Allard and Sieben (1, 2), in which two closely-spaced microphones are used to measure the sound pressures near the surface of the material. Taking into account the effect of geometric spreading, the mirror model is more accurate than the plane wave model when a monopole source is used to generate the sound field. The mirror model has been applied to two kinds of method: the transfer function method (3, 4) and the pulse-echo method (5, 6). The spherical wave model is the most accurate one among all the three models for calculating the sound field generated by a monopole above an impedance plane, especially when the distance between the sound source and the surface of the material under test is small, which is usually the case for the in-situ measurement. When using the spherical wave model, the surface impedance cannot be directly calculated from the measured acoustical quantities and an extra deduction procedure is needed (7, 8).

The methods of the second category do not depend on the type of sound wave model. A typical method of this category is the one developed by Tamura in which the spatial Fourier transform is used and the measurement of complex sound pressure distributions on two parallel planes close to the surface of the material under test is required (9, 10). In theory, the sound source can be of any type in the Tamura method, however, the sound source that is beneficial to decrease the error due to the finite size of the measurement area would be more preferable in practice, for example, a dipole source gives better results than a monopole source does. Using the Tamura method reflection coefficients for arbitrary real angles of incidence can be obtained from one set of measurements, and thus it is applicable to not only the locally reacting materials but also the non-locally reacting materials.

[1] ybzhang@hfut.edu.cn

Another advantage of the Tamura method is the fact that it can be used to measure the reflection coefficients of inhomogeneous waves.

In this paper, the equivalent source method (ESM) (10-13) is applied to measure the surface impedance and reflection coefficient of a material. The measurement procedure of the ESM-based technique is similar to that of the Tamura method, i.e., measuring complex pressures on two parallel planes located between the sound source and the test material or on two parallel lines if the sound source has rotational symmetry. But in the ESM-based technique the spatial Fourier transform is not involved. This paper is organized as follows. First the Tamura method is reviewed very briefly, and then the ESM-based measurement technique is given, followed by a short discussion of its advantages and disadvantages compared with the Tamura method. Finally numerical examples are given to demonstrate the validity of the proposed technique and for comparisons.

2. THEORY

2.1 Tamura method

Figure 1 shows the schematic illustration of the Tamura method. A sound source is placed above the material under test. Complex sound pressures are measured on two parallel planes (or lines) H_1 and H_2. By using spatial Fourier transform the incident sound field and the reflected sound field can be separated in wavenumber domain as

$$P_i(k_x,k_y,0)=\frac{P(k_x,k_y,z_1)\exp(ik_z z_2)-P(k_x,k_y,z_2)\exp(ik_z z_1)}{2i\sin[k_z(z_2-z_1)]} \tag{1}$$

$$P_r(k_x,k_y,0)=\frac{P(k_x,k_y,z_2)\exp(-ik_z z_1)-P(k_x,k_y,z_1)\exp(-ik_z z_2)}{2i\sin[k_z(z_2-z_1)]} \tag{2}$$

where (k_x,k_y,k_z) is the wave vector of the wavenumber domain, $k_z=k_0\cos\theta$, $\theta=\sin^{-1}[(k_x^2+k_y^2)^{0.5}/k_0]$ is the incidence angle of the plane wave component (k_x,k_y), k_0 is the wave number in air, $P(k_x,k_y,z_1)$ and $P(k_x,k_y,z_2)$ are spatial spectrums of sound pressures $\boldsymbol{p}_{H1}$ and $\boldsymbol{p}_{H2}$ which are measured on H_1 and H_2.

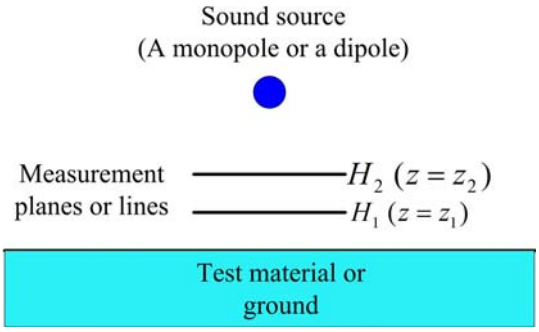

Figure 1 – Schematic illustration of the Tamura method

It can be seen from Eqs. (1) and (2) that the incident sound field and the reflected sound field on the surface of the material are decomposed into plane-wave components. The traveling direction of each plane wave component is indicated by the wave vector (k_x, k_y, k_z) or by the incidence angle θ. The reflection coefficient at an angle of incidence θ can be obtained by the following equation:

$$R_T(\theta)=P_r(k_x,k_y,0)/P_i(k_x,k_y,0)\,. \tag{3}$$

Furthermore the surface impedance is

$$Z_S^T(\theta)=\frac{Z_0}{\cos\theta}\frac{1+R_T(\theta)}{1-R_T(\theta)}\,. \tag{4}$$

where $Z_0=\rho_0 c_0$ is the characteristic impedance of air, ρ_0 is the density of air, and c_0 is the

sound speed in air.

2.2 Measurement technique based on ESM

Figure 2 shows the schematic illustration of the ESM-based method. The measurement procedure is similar to that of the Tamura method, but the ESM instead of the spatial Fourier transform is used to calculate the reflection coefficient and surface impedance. According to the ESM (10-13), the sound pressure on measurement planes (or lines) H_1 and H_2 can be represented as the superposition of sound pressures generated by equivalent sources distributed around the sound source and its image source, i.e.,

$$\begin{bmatrix} \boldsymbol{p}_{H1} \\ \boldsymbol{p}_{H2} \end{bmatrix} = \begin{bmatrix} \boldsymbol{G}_{Q1H1} & \boldsymbol{G}_{Q2H1} \\ \boldsymbol{G}_{Q1H2} & \boldsymbol{G}_{Q2H2} \end{bmatrix} \begin{bmatrix} \boldsymbol{Q}_1 \\ \boldsymbol{Q}_2 \end{bmatrix}, \tag{5}$$

where the column vectors $\boldsymbol{Q}_2$ and $\boldsymbol{Q}_1$ are strengths of equivalent sources used to replace the sound source and its image source, respectively, $\boldsymbol{G}_{QjHi}$ ($i = j = 1, 2$) is the transfer matrix relating the equivalent sources distributed around the sound source or the image source to the measurement points on H_1 or H_2, $[\boldsymbol{G}_{QjHi}]_{mn} = \exp(ik_0 |\boldsymbol{r}_m - \boldsymbol{r}_n|)/(4\pi |\boldsymbol{r}_m - \boldsymbol{r}_n|)$, $\boldsymbol{r}_m$ is the position of an equivalent source, and $\boldsymbol{r}_n$ is the position of a measurement point.

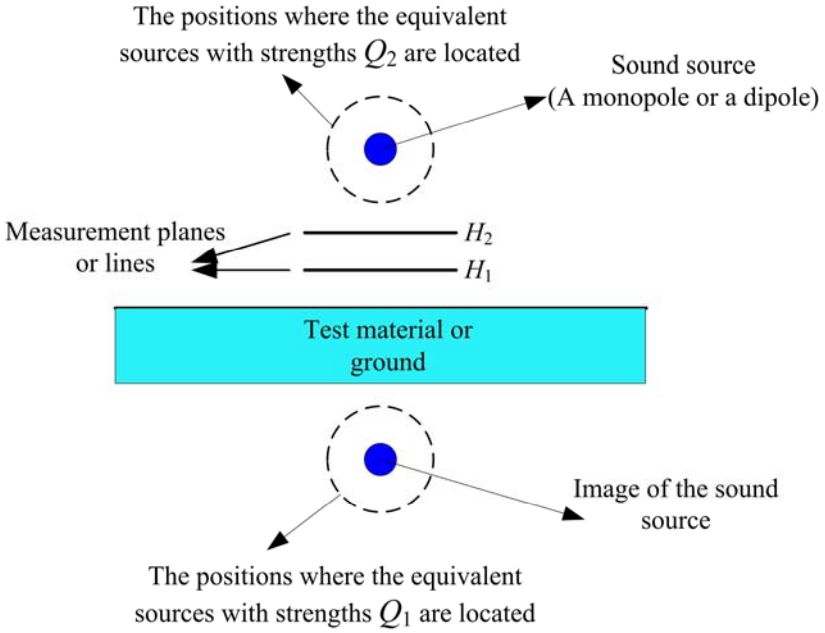

Figure 2 –Schematic illustration of the ESM-based method

Solving Eq. (5) by using singular value decomposition we can obtain the source strengths $\boldsymbol{Q}_1$ and $\boldsymbol{Q}_2$, and then the sound pressure and normal component of particle velocity at a point on the surface of the material under test can be calculated as

$$p(x, y, 0) = [\boldsymbol{G}_{Q1P0} \ \boldsymbol{G}_{Q2P0}] \begin{bmatrix} \boldsymbol{Q}_1 \\ \boldsymbol{Q}_2 \end{bmatrix}, \tag{6}$$

$$v_{z0}(x, y, 0) = \frac{1}{i\rho_0\omega} [\nabla_z \boldsymbol{G}_{Q1P0} \ \nabla_z \boldsymbol{G}_{Q2P0}] \begin{bmatrix} \boldsymbol{Q}_1 \\ \boldsymbol{Q}_2 \end{bmatrix}, \tag{7}$$

where the vector $(x, y, 0)$ denotes a point, for example $P0$, on the surface of the material, and $\nabla_z = \partial/\partial z$. The surface impedance can then be obtained by the following equation:

$$Z_S^E = \frac{p(x,y,0)}{v_{z0}(x,y,0)}. \tag{8}$$

Actually we can calculate the surface impedance of more than one point by using Eq. (8), and averaging the surface impedance at several points will give a better result if the material under test is homogeneous. However, the points that are not covered by the measurement plane should not be used because the ESM cannot ensure the accuracy of the reconstructed sound field outside the measurement aperture. After obtaining the surface impedance, the reflection coefficient at an angle of incidence θ can be obtained as

$$R_E(\theta) = \left(Z_S^E \cos\theta - Z_0\right) / \left(Z_S^E \cos\theta + Z_0\right). \tag{9}$$

2.3 Comparisons of the two methods

The common advantage of the Tamura method and the ESM-based method is the fact that they do not depend on any sound wave model, and thus have fewer requirements of the sound source characteristics such as the source strength and source position than other free field methods. The surface impedance [Eq. (4)] when plane wave component strikes the material from an arbitrary angle of incidence can be obtained by using the Tamura method, however, the ESM-based method can just provide the surface impedance [Eq. (8)] at a normal incidence. So the Tamura method can be applied to not only the locally reacting materials but also the non-locally reacting materials, whereas the ESM-based method can be applied to the locally reacting materials only. When applying the ESM-based method to non-locally reacting materials, the surface impedance obtained by Eq. (8) is an "effective" quantity and cannot reflect the influence of the angle of incidence.

In the Tamura method, due to the use of spatial Fourier transform, the size of measurement aperture is required to be large enough to reduce the error caused by the truncation effects. An alternative way is to use a sound source whose sound field decays fast toward the edges of the measurement aperture, for example, a dipole source. In the ESM-based method, the spatial Fourier transform is not involved, so the measurement aperture can be smaller than that required by the Tamura method and it is not necessary to restrict the characteristic of the sound source. As shown later in the simulation part, the result of the ESM-based method is acceptable when using a monopole source.

Different from the conventional near-field acoustic holography (NAH), there is no inverse spatial Fourier transform involved in the Tamura method. When the measured sound pressure contains noise, it is difficult to control their influence because the spatial spectrum will be distorted if we apply a low-pass wavenumber domain filter to Eqs. (1) and (2). In addition, the reflection coefficient at real angle of incidence corresponds to wavenumbers small than k_0, and the measurement noise distributed inside the radiation circle cannot be controlled effectively even if a low-pass filter is used. On the contrary, in the ESM-based method it is easy to deal with the influence of measurement noise by using the Tikhonov regularization when calculating the source strengths $\boldsymbol{Q}_1$ and $\boldsymbol{Q}_2$ from Eq. (5).

3. NUMERICAL SIMULATION

The material under test is assumed to be of the Delany and Bazley type (14), i.e., the characteristic impedance of the test material is

$$Z = Z_0[1 + 9.08(f/\sigma)^{-0.75} - i11.9(f/\sigma)^{-0.73}], \tag{10}$$

where σ is the flow resistivity and is 50 cgs units in the following simulations. And we assume that the test material has an infinite thickness. As shown in Fig. 3, the sound source (both the monopole source and dipole source were examined) was placed at a height 10 cm above the material, the sound field was measured on two parallel lines along *y*-axis which were 1 cm and 3 cm above the surface of the material. In the Tamura method the measurement lines started from the *z*-axis (i.e., *y*=0) and ended at the position where *y*=1 m, the sampling space was 0.01m, thus providing 101 points on each line. In the ESM-based method the measurement lines started also from the *z*-axis (i.e., *y*=0) but ended at the position where *y*=0.1 m, the sampling space was still 0.01m, thus providing 11 points on each line. Because the sound source used in the simulation has axial symmetry with respect to *z*-axis, the measured sound pressure can be extended to 21 points (from *y*= -0.1 m to 0.1 m) in the ESM-based method and to 201 points (from *y*= -1 m to 1 m) in the Tamura method. However, as observed in simulations, this kind of extension can obviously improve the performance of the ESM-based method, but has no distinct influence on the Tamura method because the spatial spectrum

was calculated by Fourier-Bessel transform. In the ESM-based method, the equivalent sources were allocated on circles (see Fig. 2), the center of the circles were located at positions of the sound source and its image source, the radii of the circles were 1 cm, and there were 12 points evenly distributed on each circle. When noise (white Gaussian noise corresponding to a signal-to-noise ratio of 30 dB) was added to the measured pressure, the Tikhonov regularization was used in the ESM-based method and the regularization parameter was chosen by the L-curve method (15).

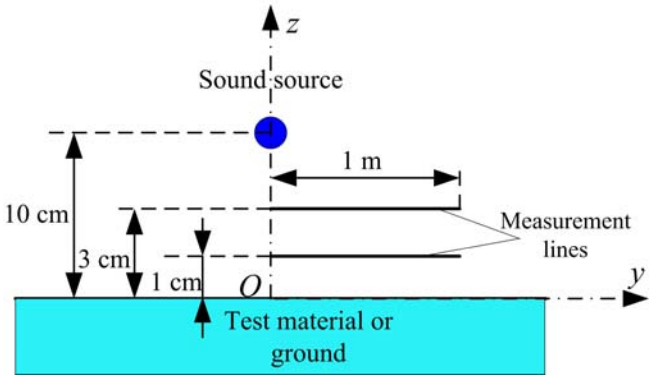

Figure 3 –Schematic illustration of the measurement

3.1 Monopole case

The sound field generated by a monopole source was calculated according to the method proposed by Di and Gilbert (16). In Table 1 the normalized surface impedances calculated by the ESM-based method and Tamura method are compared with true values obtained from the Delany and Bazley model. The cases without and with considering measurement noise were both examined in the ESM-based method, and in the Tamura method measurement noise was not considered since there was not an effective way to control the influence of noise. According to Eq. (4) we can obtain the surface impedance when the plane wave strikes the material from an arbitrary angle of incidence, and if the material under test is of locally reacting type, the surface impedance corresponding to different angle of incidence should be close to each other. The results of Tamura method presented in Table 1 are the ones when the angle of incidence was 0° (i.e. at normal incidence). As shown in Table 1, there is a good agreement between the results of ESM-based method and the true values, no matter whether the measurement noise was considered or not. However, the results of Tamura method do not agree with the true values well, and the extent of agreement between them become even worse with the increase of frequency.

Table 1 –Comparison of normalized surface impedance when a monopole source was used

Frequency (Hz)	500	1000	2000	4000
D-B model	2.61 - 2.22i	1.96 - 1.34i	1.57 - 0.81i	1.34 - 0.49i
ESM/without noise	2.88 - 2.31i	2.09 - 1.39i	1.63 - 0.82i	1.36 - 0.47i
ESM/with noise (30 dB)	2.70 - 2.58i	2.11 - 1.57i	1.63 - 0.91i	1.35 - 0.50i
Tamura/without noise	1.95 - 1.92i	1.5 - 1.86i	1.17 - 0.53i	0.67 - 0.66i

Figure 4 shows the reflection coefficients *versus* the angle of incidence at 1000 Hz when a monopole source was used. It can be seen that the results of ESM-based method agree well with the true values calculated from the Delany and Bazley model. However, although the size of measurement aperture of the Tamura method was ten times larger than that of the ESM-based method, the results of Tamura method, especially the imaginary parts of reflection coefficients, have distinct fluctuations. This is because the measurement aperture was not large enough and additional errors were resulted in due to the truncation effect in the Tamura method.

The results of this case show that the ESM-based method is feasible and effective in measuring the surface impedance and reflection coefficients of a material, and is less affected by the truncation effect compared with the Tamura method. In addition, it is possible to consider measurement noise in

the ESM-based method.

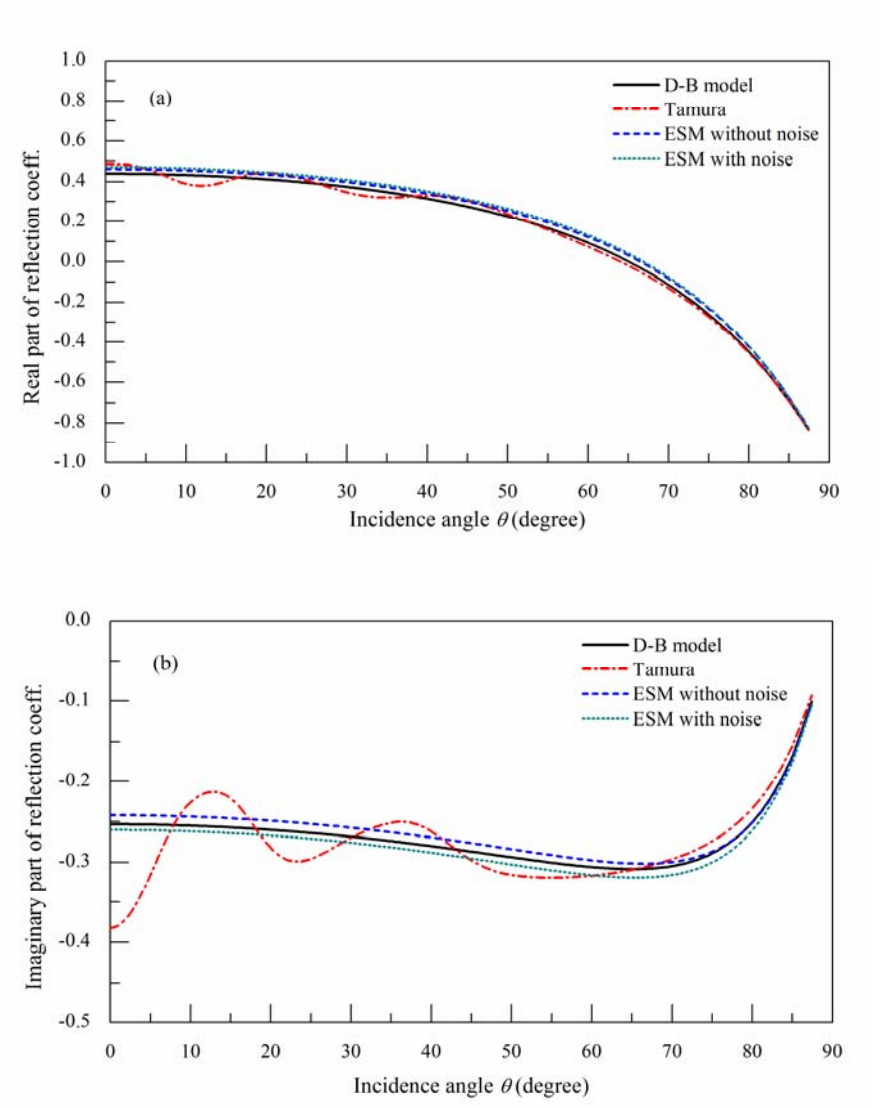

Figure 4 –Real part (a) and imaginary part (b) of reflection coefficient *versus* angle of incidence at 1000 Hz. A monopole source was used and the flow resistivity σ was 50 cgs units.

3.2 Dipole case

The axis of the dipole was along the z-axis, the sound field of which was calculated following the way used by Tamura, i.e., applying the inverse Fourier transform to the spatial spectrum of a dipole.

Table 2 –Comparison of normalized surface impedance when a dipole source was used

Frequency (Hz)	500	1000	2000	4000
D-B model	2.61 - 2.22i	1.96 - 1.34i	1.57 - 0.81i	1.34 - 0.49i
ESM/without noise	2.64 - 2.20i	1.92 - 1.33i	1.53 - 0.82i	1.31 - 0.51i
ESM/with noise (30 dB)	2.68 - 2.67i	1.96 - 1.32i	1.54 - 0.84i	1.33 - 0.52i
Tamura/without noise	2.75 - 2.07i	1.83 - 1.32i	1.62 - 0.69i	1.21 - 0.46i

In Table 2 the normalized surface impedances calculated by the ESM-based method and Tamura method are compared with true values obtained from the Delany and Bazley model. The results of Tamura method presented in Table 2 are also the ones when the angle of incidence was 0°. It can be seen that there is a good agreement among the results of ESM-based method, the results of Tamura

method and the true values. Figure 5 shows the reflection coefficients *versus* the angle of incidence at 1000 Hz when a dipole source was used. It can be seen that there is still a good agreement between the results of ESM-based method and the true values, and the results of Tamura method are improved significantly when a dipole source instead of a monopole source was used.

The results of this case show that both the ESM-based method and the Tamura method perform well when a dipole source is used, but it should be noted that the size of measurement aperture of the ESM-based method in this simulation was much smaller than that of the Tamura method.

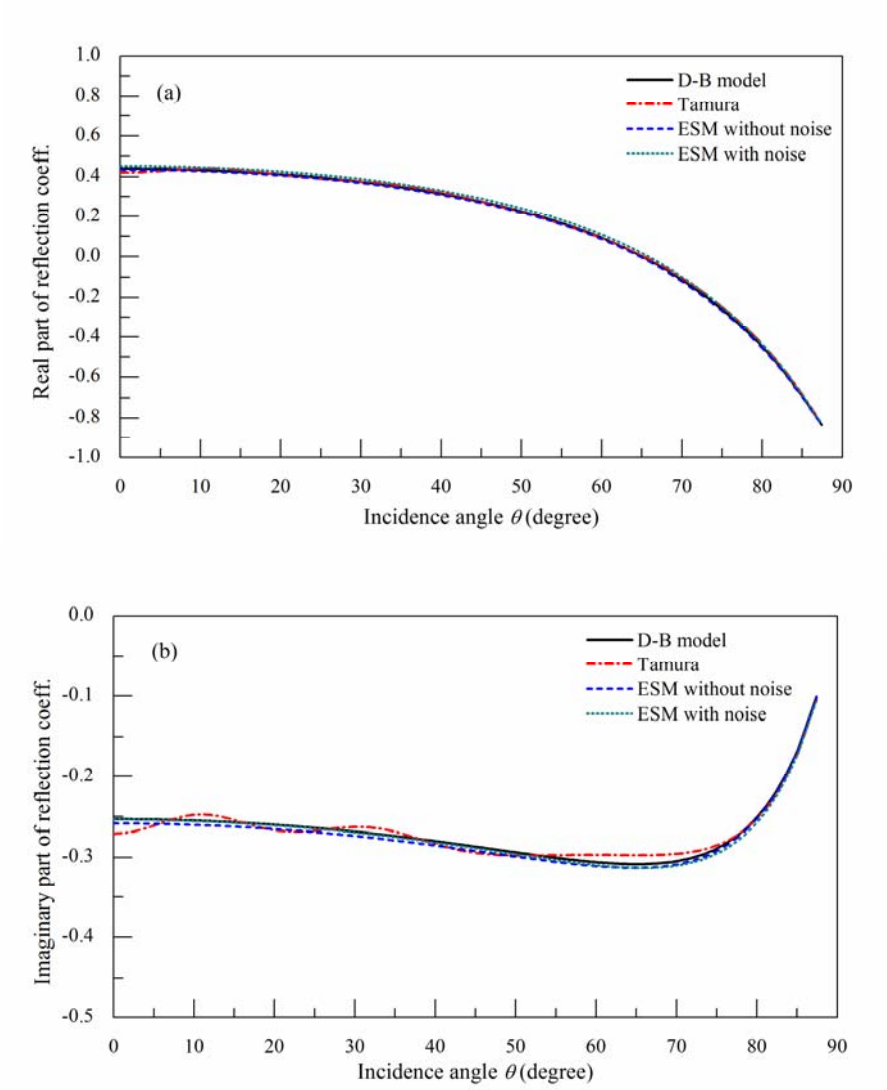

Figure 5 –Real part (a) and imaginary part (b) of reflection coefficient *versus* angle of incidence at 1000 Hz. A dipole source was used and the flow resistivity σ was 50 cgs units.

4. CONCLUSIONS

This paper presented a method for measuring the surface impedance and reflection coefficients of a material under test based on the equivalent source method (ESM). The ESM-based method does not depend on any sound wave model such as the plane wave model, the mirror model or the spherical wave model, which is similar to the method proposed by Tamura. The ESM-based method was examined by numerical simulations, and the results show that the proposed method is feasible and effective in measuring the surface impedance or reflection coefficients of a material.

The ESM-based method was compared with the Tamura method theoretically and numerically, and the following conclusions have been obtained. The Tamura method can be applied to not only the locally reacting materials but also the non-locally reacting materials, whereas the ESM-based method can be applied to the locally reacting materials only. When applying the ESM-based method

to non-locally reacting materials, the obtained surface impedance is an "effective" quantity and cannot reflect the influence of the angle of incidence. The ESM-based method is less affected by the truncation effect than the Tamura method because the spatial Fourier transform is not involved, and thus the measurement aperture when using the ESM-based method could be much smaller than that when using the Tamura method. The measurement noise can be directly suppressed by Tikhonov regularization in the ESM-based method, but in the Tamura method there is not an effective way to control measurement noise.

ACKNOWLEDGEMENTS

This work was supported by National Natural Science Foundation of China (Grant Nos. 51322505 and 11274087).

REFERENCES

1. Allard JF, Sieben B. Measurement of acoustic impedance in a free field with two microphone and a spectrum analyzer. J. Acoust. Soc. Am. 1985; 77: 1617-1618.
2. Allard JF, Bourdier R, Bruneau AM. The measurement of acoustic impedance at oblique incidence with two microphones. J. Sound Vib. 1985; 101: 130-132.
3. Lanoye R, Vermeir G, Lauriks W. Measuring the free field acoustic impedance and absorption coefficient of sound absorbing materials with a combined particle velocity-pressure sensor. J. Acoust.Soc. Am. 2006; 119: 2826-2831.
4. Alvarez Balderrama JD. In situ measurement of the complex acoustic impedance of materials for automobile interiors. MSc thesis, Technical University of Denmark; 2006.
5. Garai M. Measurement of the sound absorption coefficient in situ: the reflection method using periodic pseudo-random sequences of maximum length. Appl. Acoust. 1993; 39, 119-39.
6. Mommertz E. Angle-Dependent in-situ measurements of reflection coefficients using a subtraction technique. Appl. Acoust. 1995; 46: 251-263.
7. Nock C, Mellert V. Impedance deduction from broad-band, point-source measurements at grazing incidence. Acta Acust. Acust. 1997; 83: 1085-1090.
8. Hess HM, Attenborough K, Heap NW. Ground characterization by short-range propagation measurements. J.Acoust.Soc. Am. 1990; 87: 1975-1986.
9. Tamura M. Spatial Fourier transform method of measuring reflection coefficients at oblique incidence. I: Theory and numerical examples. J .Acoust. Soc. Am. 1990; 88: 2259-2264.
10. Tamura M. Spatial Fourier-transform method for measuring reflection coefficients at oblique incidence. II: Experimental results. J .Acoust. Soc. Am. 1995; 97: 2255-2262.
11. Koopmann GH, Song L, Fahnline J. A method for computing acoustic fields based on the principle of wave superposition. J. Acoust. Soc. Am. 1989; 86: 2433-2438.
12. Ochmann M. The source simulation technique for acoustic radiation problems. Acustica 1995; 81: 512-527.
13. Zhang YB, Jacobsen F, Bi CX, Chen XZ. Near field acoustic holography based on the equivalent source method and pressure-velocity transducers. J. Acoust. Soc. Am. 2009; 126: 1257-1263.
14. Delany ME, Bazley EN. Acoustical characteristics of fibrous absorbent materials. Appl. Acoust. 1970; 3: 105-116.
15. Hansen PC, O' Leary DP. The use of the L-curve in the regularization of discrete ill-posed problems. SIAM J. Sci. Comput. 1993; 14: 1487-1503.
16. Di X, Gilbert KE. An exact Laplace transform formulation for a point source above a ground surface. J. Acoust. Soc. Am. 1993; 93: 714-720.